

On the dynamics of proto-neutron star winds and r-process nucleosynthesis

I.V. Panov^{1,2} and H.-Th. Janka¹

¹ Max-Planck-Institut für Astrophysik, Karl-Schwarzschild-Straße 1, D-85740 Garching, Germany

² Institute for Theoretical and Experimental Physics, B. Chermushkinskaya 25, Moscow, 117259, Russia.

Preprint online version: November 30, 2018

ABSTRACT

We study here the formation of heavy r-process nuclei in the high-entropy neutrino-driven wind environment. In particular, we explore the sensitivity of the element creation in the $A \gtrsim 130$ region to the low-temperature behavior of the outflows. For this purpose we employ a simplified model of the dynamics and of the thermodynamical evolution for radiation dominated, adiabatic outflows. It consists of a first stage of fast, exponential cooling with timescale τ_{dyn} , followed by a second phase of slower evolution, either assuming constant density and temperature or a power-law decay of these quantities. This behavior is supposed to capture the most relevant effects associated with a deceleration of supersonic winds caused by the collision with the slower, preceding supernova ejecta and the corresponding presence of a wind termination shock. We find that for given entropy, expansion timescale, and proton-to-baryon ratio not only the transition temperature between the two expansion phases can make a big difference in the formation of the platinum peak, but also the detailed cooling law during the later phase. Because the nuclear photodisintegration rates between about 2×10^8 K and roughly 10^9 K are more sensitive to the temperature than the neutron-capture rates are to the free neutron density, a faster cooling but continuing high neutron density in this temperature regime allow the r-process path to move closer to the neutron-drip line. With low (γ, n) - but high β -decay rates, the r-processing does then not proceed through a (γ, n) - (n, γ) equilibrium but through a quasi-equilibrium of (n, γ) -reactions and β -decays, as recently also pointed out by Wanajo. Unless the transition temperature and corresponding (free neutron) density become too small ($T \lesssim 2 \times 10^8$ K), a lower temperature or faster temperature decline during the slow, late evolution phase therefore allow for a stronger appearance of the third abundance peak.

Key words. Nuclear reactions, nucleosynthesis, abundances — Stars: supernovae: general — Stars: winds, outflows — Stars: neutron

1. Introduction

Heavy nuclei beyond the iron peak are known to be produced in nature mainly through neutron capture reactions (Burbidge et al. 1957). Rapid neutron capture and the reverse photodisintegration processes achieve an equilibrium among the isotopes of each heavy element. Then beta-decay occurs that leads to the increase of the nuclear charge and formation of a new element. When the neutron capture rate is much higher than the beta-decay rate ($\lambda_{n\gamma} > \lambda_{\beta}$) and $T_9 \sim 1$, the r-process can start and, for a sufficiently high neutron-to-seed ratio, the wave of nucleosynthesis drives the process to heavier nuclei, forming, in part, the abundance r-process peaks at ~ 80 , 130 and 196.

Although the r-process sites remain unknown, many astrophysical models and sources for r-process elements have been proposed during the last 50 years, including, in particular, such scenarios as that of an explosion on a neutron-star surface (Bisnovatyι-Kogan and Chechetkin 1979), a collision of a neutron star with a black hole (Lattimer & Schramm, 1976), an explosion of a low-mass neutron star (Imshennik, 1992), and the hypothetical escape of nucleon bubbles in case of a soundless stellar collapse (Imshennik & Litvinova 2006). The latter scenario was suggested as origin

of gamma-ray bursts but could also be an interesting site for the nucleosynthesis of heavy elements.

Presently, however, it seems most likely that rapid n-capture nucleosynthesis can take place during different stages of supernova explosions (e.g., Hillebrandt 1978; Woosley & Hoffman 1992), or in neutron star mergers (e.g., Lattimer & Schramm 1974; Symbalιsty & Schramm 1982; Freiburghaus et al. 1999). An overview of the currently discussed possible sites is given in a recent review paper by Arnould et al. (2007).

Supernovae and neutron star mergers have different advantages and weak points, but the main difference lies probably in the initial neutron-to-proton ratio, which is necessary to support a sufficiently high free neutron density during several hundreds of milliseconds. With respect to this parameter, all astrophysical scenarios can be separated into two distinct groups, in which nucleosynthesis can be carried out over short or long timescales (so-called short-time or long-time solutions, respectively), as introduced by Seeger et al. (1965). In nature, the r-process might be realized in both these types of sources and also other ones might contribute (see for example Cameron, 2003; Arnould et al. 2007). It is only future modelling and observations that will be able clarify the multiplicity of the r-process models and types, as well as the contributions from different produc-

tion sites to the r-process element abundances observed in the Solar System.

Among the astrophysical events proposed as sites for the r-process, supernova explosions still remain the preferable ones (see, e.g., Wanajo & Ishimaru 2006, and references therein). In particular, supernova explosions can distribute r-process material all over the Galaxy, and estimated amounts of heavy elements produced in SN explosions are in accordance with the observations.

The neutrino-driven wind from a hot neutron star produced in a supernova explosion has been considered as a probable site for the r-process by many authors (see *e.g.* Meyer et al. 1992; Woosley et al. 1994; Wittl et al. 1993; Otsuki et al. 2000; Sumiyoshi et al. 2000; Terasawa et al. 2001; Wanajo et al. 2001). A part of the surface material of a neutron star is heated by the supernova neutrinos and gets ejected. It can be described as a hot outflow with a fairly high entropy and a moderate density.

Various studies of the r-process element formation in proto-neutron star winds have been conducted during the past years. Hoffman, Woosley & Qian (1997), employing the analytic wind model of Qian and Woosley (1996), explored the possibility of third peak creation for different combinations of the determining parameters of Y_e , entropy, and expansion timescale. Altogether, they showed (see their Fig. 10) that for typical values of $Y_e \gtrsim 0.4$ in the wind the third r-process peak can be produced for combinations ranging from moderate entropy ($s \sim 100$ in units of Boltzmann’s constant per baryon) and very short timescales (t_{exp} a few milliseconds) to high entropies ($s \gtrsim 400$) and long expansion timescales (a few 100 milliseconds). The wind models existing at that time failed to provide the necessary conditions (Wittl et al. 1994, Qian and Woosley 1996).

Subsequently, several other studies of neutrino-driven winds in the framework of general relativistic gravity (Otsuki et al. 2000, Sumiyoshi et al. 2000, Thompson et al. 2001, Wanajo et al. 2001, 2002) confirmed the need of fairly extreme conditions concerning expansion timescale or entropy for strong r-processing up to $A \sim 200$. Since very high entropies could not be obtained in the wind scenario or were found to be associated with too low mass loss rates for any significant production of r-nuclei, these studies also demonstrated a preference for the case of moderate entropies, $s \sim 100\text{--}200$, and very short timescales. This seemed to give a bias for winds from compact neutron stars with a large mass, $M \gtrsim 2M_\odot$, and a small radius $R \lesssim 10$ km as the most likely site for r-process element formation up to the platinum peak.

This conclusion was found to hold independent of whether freely expanding, transsonic “wind” outflows were considered (Hoffman et al. 1997, Thompson et al. 2001) or subsonic “breeze” solutions (Otsuki et al. 2000; Sumiyoshi et al. 2000; Wanajo et al. 2001, 2002; Terasawa et al. 2001, 2002). The former are characterized by a monotonically increasing velocity and a continuous temperature decrease when the radius goes to infinity, whereas the latter are obtained when a chosen, non-vanishing value of the pressure and temperature is required to be reached at the outer boundary at some large radius (this is supposed to mimic the fact that the fast neutrino-driven wind is decelerated again as it collides and merges with the preceding, more slowly expanding material ejected in the early phase of the supernova blast). In fact, the results from both types of

outflow scenarios turned out to be in very good quantitative agreement (compare, e.g., Fig. 11 in Thompson et al. 2001 with Fig. 8 in Otsuki et al. 2000 and with Table 2 and Fig. 6 in Sumiyoshi et al. 2000).

Later Terasawa et al. (2002) announced to have found successful conditions even for proto-neutron stars with a more typical mass around $1.4M_\odot$ and a radius of 10 km. Like previous studies (in particular Sumiyoshi et al. 2000, but also Otsuki et al. 2000) they considered breeze outflows, but different from the earlier investigations they chose a smaller value for the outer boundary pressure, which implied a lower asymptotic temperature. They argued that this is favorable for a strong r-processing up to the third peak because the lower final temperature is associated with a faster expansion and more rapid cooling. The more quickly decreasing temperature leads to a slowing down of charged-particle reactions and reduces the efficiency of α -particle recombination. Therefore it leads to less production of seed nuclei and a higher neutron-to-seed ratio. Such a sensitivity to the expansion timescale was also seen by Arnould et al. (2007), who performed systematic variations of the parameters in analytic wind and breeze solutions. Arnould et al. (2007) verified that wind solutions provide the more favorable conditions for strong r-processing than the slower breezes, because for given values of the entropy and mass loss rate the expansion timescale is directly correlated with the asymptotic value of the temperature and thus of the total specific energy of the outflowing gas. These values are lowest in case of freely expanding winds. Arnould et al. (2007), however, also saw that the mass loss rate has a much more sensitive influence: breeze solutions with higher mass loss rates (and otherwise the same characterising parameter values) make a faster expansion and allow for a stronger r-process despite having higher asymptotic values of the temperature.

Although Arnould et al. (2007) confirmed the formation of the third r-process peak for combinations of entropy, expansion timescale, Y_e , neutron star mass, and asymptotic temperature in the ballpark of those considered by Terasawa et al. (2002), the results of the latter paper are nevertheless in contradiction to the earlier studies by Otsuki et al. (2000), Sumiyoshi et al. (2000), and Thompson et al. (2001): Terasawa et al. (2002) obtained a significantly higher entropy and shorter expansion timescale than Sumiyoshi et al. (2000) even for the same choice of outflow determining conditions, i.e., for the same individual neutrino luminosity ($L_{\nu_i} = 10^{51}$ ergs $^{-1}$), the same mean neutrino energies, and in particular the same outer boundary pressure (compare Table 1 in the Terasawa et al. work and Section 3.2 in Sumiyoshi et al.). Moreover, for all tested values of the boundary pressure, Terasawa et al. (2002) found outflow properties for their $1.4M_\odot$ neutron star that were largely different from those plotted for breezes in Fig. 8 of Otsuki et al. (2000) and for freely expanding winds in Fig. 11 of Thompson et al. (2001). These differences seem to have been causal for the successful solar system like r-process reported by Terasawa et al. (2002), but the actual reason why the more favorable outflow behavior was obtained, remains unexplained¹.

¹ Note that Thompson et al. (2001) used a sophisticated description of the equation of state and thus explicitly accounted for the nonrelativistic character of electrons and positrons at low temperatures, an effect that Sumiyoshi et al. (2000) pointed out

Recently, Arcones et al. (2007) performed new hydrodynamic simulations of neutrino-driven winds, systematically exploring the effects of the wind termination shock that forms when the supersonic wind collides with the slower earlier supernova ejecta (Janka & Müller 1995a,b; Burrows et al. 2005; Buras et al. 2006, see also Tomás et al. 2004) and that decelerates the outflow abruptly. They found that the position of the reverse shock is strongly dependent on the evolution phase, progenitor structure, and explosion energy of the supernova. Motivated by these studies, interest has recently turned to a closer exploration of the relevance of the late-time wind dynamics for r-process nucleosynthesis. On the one hand, Wanajo (2007) discovered that a solar-like r-process can also be produced in supersonically expanding outflows whose temperature drops quickly to a few 10^8 K instead of asymptoting to a value around 10^9 K as previously mostly assumed (Otsuki et al. 2000, Sumiyoshi et al. 2000, Wanajo et al. 2001, 2002). In such a low-temperature environment an (n, γ) - (γ, n) equilibrium is never achieved during the nucleosynthesis of heavy r-process material, but neutron captures compete with β -decays in the low-density matter, similar to what was discussed by Blake & Schramm (1976).

On the other hand, Kuroda et al. (2008) started to explore for the first time systematically the consequences of the wind termination shock for the r-processing in the wind. Decelerating the outflow abruptly, the reverse shock does not only raise the entropy of the matter, but in particular it slows down the temperature and density decline that takes place in the subsequent expansion. Kuroda et al. (2008) found that the change of the temperature behavior plays a decisive role in determining the r-process abundances, because the nucleosynthesis path depends strongly on the temperature during the r-process freeze-out phase. In contrast, the entropy jump does not seem to be important because high entropies in the shocked outflows are reached only when the temperature is already well below 2.5×10^9 K, i.e. not in the regime where the neutron-to-seed ratio is established before the onset of r-processing.

In the present paper we also investigate the influence of the late-time outflow dynamics on the r-process nucleosynthesis. To this end we consider outflow trajectories that consist of an initial homologous phase and a second, slower expansion stage. This describes the wind dynamics only schematically but at least some basic features that are found in detailed solutions of shocked outflows can be reproduced. In contrast to the outflow solutions studied by Arnould et al. (2007), for example, our simple parametric ansatz for the temperature and density decrease in the ejected matter allows us to modify the early expansion behavior and that at late times independently, i.e. in an uncoupled way. This is closer to how the presence of a wind termination shock acts on the matter. Motivated by the insensitivity to the entropy jump seen by Kuroda et al. (2008), we ignore the discontinuity of the fluid variables at the location where their time dependence is assumed to change.

Our paper is structured as follows. In Sect. 2 we will describe the dynamical model and the network used in our study, and will present some numerical tests we performed.

In Sect. 3 we will describe our results and in Sect. 4 we finish with conclusions.

2. Network, input data, and numerical modelling of the $(\alpha+r)$ -process

We consider here the conditions for r-process nucleosynthesis in neutrino-driven outflows from the surface layers of hot nascent neutron stars, which have been the subject of many previous studies, where different aspects of the problem were discussed (see, e.g., Qian & Woosley 1996; Hoffman et al. 1997; Woosley et al. 1994; Cardall & Fuller 1997; Qian & Wasserburg 2000; Takahashi et al. 1994; Otsuki et al. 2000; Sumiyoshi et al. 2000; Thompson et al. 2001; Kuroda et al. 2008, Arnould et al. 2007, and references therein). Our main goal here is to evaluate numerically the possibility of producing r-process elements in this environment in dependence of the late-time behavior of the outflowing gas. Within the framework of a very simple, purely analytic model we want to determine the favorable combinations of entropy, Y_e and dynamical timescale, and how sensitively these parameters influence the outcome. Our parametric approach has the advantage of reducing the dynamical aspects of the problem to an absolute minimum of ingredients, giving one much freedom in the choice of the involved parameter values. However, it clearly has the disadvantage that our results are at most indicative of what might be seen in nucleosynthesis calculations based on more sophisticated models of the outflow dynamics. Moreover, of course, our results will not allow us to make a judgement about whether neutrino-driven winds are the long-sought site of r-process material or not.

We represent the outflow behavior during the early and late expansion phases by different analytic functions, which qualitatively (but certainly not to a high accuracy) describe the wind acceleration through the sonic point on the one hand, and the evolution of the outflow after its deceleration by a reverse shock on the other hand.

In the first stage of the expansion of a spherical mass shell we assume a homologous velocity-radius dependence, $v \propto r$, corresponding to an exponential growth of the radius, $r(t) = R_{\text{ini}} \exp(t/\tau_{\text{dyn}})$. Therefore, steady-state conditions (which imply $r^2 \rho v = \text{const}$) yield an exponential decline of the density and for an adiabatically expanding, radiation-dominated wind (i.e., $\rho \propto T^3$) also an exponential decrease of the temperature:

$$\rho(t) = \rho_{\text{ini}} \cdot \exp(-3t/\tau_{\text{dyn}}), \quad (1)$$

$$T_9(t) = T_9^{\text{ini}} \cdot \exp(-t/\tau_{\text{dyn}}). \quad (2)$$

Here T_9 is the temperature normalized to 10^9 K and ρ_{ini} and T_9^{ini} are the initial values of density and temperature at some small radius R_{ini} . The dynamical timescale or expansion timescale τ_{dyn} will be treated as a free parameter and can vary between 1 ms and more than 100 ms.

For reasons of simplicity, we will always assume that ρ is proportional to T^3 and that the gas entropy per nucleon (in units of Boltzmann's constant k_B) is given by the relation $s = 3.34 T_9^3 / \rho_5$ with $\rho_5 = \rho / (10^5 \text{ g cm}^{-3})$. One should, however, keep in mind that this is only a simplifying approximation, which is accurate only when the entropy of the gas is sufficiently large ($s \gtrsim 100 k_B$ per nucleon) and the temperature sufficiently high ($T_9 \gtrsim 5$). In this case

to be important for a reliable determination of the expansion timescale.

radiation-dominated conditions prevail, electrons are relativistic, electron-positron pairs are abundant, and baryons contribute to the total entropy only at the level of a few percent. In reality, however, the pairs begin to disappear below $T_9 \approx 5$ and the ratio T^3/ρ increases. Assuming it to be constant also at low temperatures therefore leads to an overestimation of the density in the outflowing matter compared to a truly adiabatic evolution (see Wittl et al. (1994) for a detailed discussion).

The deceleration by the reverse shock is supposed to happen at a radius r_0 and time t_0 when the velocity, density, and temperature reach the values v_0 , ρ_0 , and T_0 , respectively. As discussed in the introduction, we ignore here the discontinuous behavior of the dynamical and thermodynamical variables at the shock and connect the early-time behavior continuously with the late-time behavior. This means that also the ratio T^3/ρ (and therefore the quantity s that we consider as gas entropy) remains unchanged at the transition point and is taken to be constant during the following second stage of the expansion. For the latter we consider two cases with different limiting behavior for $t \gg t_0$. In the first case we assume that the density and temperature asymptote to constant values,

$$\rho(t) = \rho_0, \quad (3)$$

$$T(t) = T_0, \text{ for } t \geq t_0. \quad (4)$$

For steady-state conditions this implies that the radius and the velocity of a Lagrangian mass shell evolve at $t \geq t_0$ according to

$$r(t) = r_0 \left[1 + 3 \frac{v_0}{r_0} (t - t_0) \right]^{1/3}, \quad (5)$$

$$v(t) = v_0 \left[1 + 3 \frac{v_0}{r_0} (t - t_0) \right]^{-2/3}, \quad (6)$$

and therefore $r(t) \propto t^{1/3}$ and $v(t) \propto t^{-2/3} \rightarrow 0$ for $t \gg t_0$. In the second investigated case the density and temperature are still assumed to decline at late times, but much less steeply than during the exponential first expansion phase:

$$\rho(t) = \rho_0 \left(\frac{t}{t_0} \right)^{-2}, \quad (7)$$

$$T(t) = T_0 \left(\frac{t}{t_0} \right)^{-2/3}, \text{ for } t \geq t_0. \quad (8)$$

For steady-state conditions this corresponds to

$$r(t) = r_0 \left[1 - \frac{v_0 t_0}{r_0} + \frac{v_0 t_0}{r_0} \left(\frac{t}{t_0} \right)^3 \right]^{1/3}, \quad (9)$$

$$v(t) = v_0 \left[1 - \frac{v_0 t_0}{r_0} + \frac{v_0 t_0}{r_0} \left(\frac{t}{t_0} \right)^3 \right]^{-2/3} \left(\frac{t}{t_0} \right)^2, \quad (10)$$

which yields $r(t) \propto t$ and $v(t) = v_0^{1/3} (r_0/t_0)^{2/3} = \text{const} > 0$ for $t \gg t_0$. Note that $v(t \rightarrow \infty) < v_0$, i.e. deceleration (and not only a slow-down of the expansion) happens, if $t_0 > \tau_{\text{dyn}}$. Values of the parameters used for some of the considered model cases are listed in Table 1.

At the onset of its expansion, the ejected matter in the neutrino-driven wind is very hot and composed of free neutrons and protons. With ongoing cooling the nuclear statistical equilibrium (NSE) shifts towards an increasing mass

fraction of alpha particles until finally the recombination to heavy nuclei sets in. Provided the conditions of entropy, electron fraction, and expansion timescale are suitable, the production of elements between the first and second peaks of the abundance curve through charged particle reactions and neutron captures may occur. For sufficiently extreme conditions even third-peak elements and ($A \sim 196$) may be assembled. Typically starting our nucleosynthesis calculations at temperatures $T_9 \sim 6$ and densities $\rho \sim 10^5 - 10^6 \text{ g cm}^{-3}$, the element formation in our model runs first proceeds mainly through charged-particle reactions. As the temperature and density decrease, the importance of (α, X)- and inverse reactions diminishes and the nuclear flow begins to be driven by a dynamical r-process, provided a sufficient number of free neutrons is still present. The production of some mass fraction of heavy nuclei with $Z \geq 26$ before the onset of rapid neutron captures significantly reduces the requirements for the neutron source (a smaller number of free neutrons is required).

The time-dependent concentrations of nuclear species, $Y(A, Z)$, during the r-processing as determined by reactions with neutrons, beta-decays, and fission processes are described by the nucleosynthesis network developed by Blinnikov & Panov (1996) and Nadyozhin et al. (1998). This network was here extended by charged-particle reactions and a larger number of nuclear reactions and fission processes so that it is possible to handle both the initial α -process and the subsequent r-process with the same code.

The number of nuclei and reaction equations included in calculations depends on boundary conditions and the employed nuclear mass model and can be as large as about 4300. We considered the region of nuclei with Z ranging from 3 to 100. The minimum and maximum atomic mass values for each chemical element were determined by the proton and neutron drip lines.

The reaction rates entering the system of differential equations differ by tens of orders of magnitude. Thus, the system of equations for nuclear kinetics to be solved is a classical example of a stiff system of ordinary differential equations. We used one of the most effective methods to integrate such a stiff system of equations, Gear's method (Gear, 1971). The description of the complete package of solver routines and its applications to the r-process calculations can be found in Nadyozhin et al. (1998).

Nuclear mass values as predicted by FRDM (Kratz et al. 1993) were used, the beta-decay rates were calculated in the framework of the QRPA-model (Kratz et al. 1993), and the reaction rates with neutrons were described according to the calculations of Cowan et al. (1991) and of Rauscher & Thielemann (2000).

In the nucleosynthesis studies presented here, the triple α and $\alpha\alpha n$ reactions of helium burning, $3\alpha \rightarrow {}^{12}\text{C}$ and $\alpha + \alpha + n \rightarrow {}^9\text{Be}$, respectively, along with their inverse reactions, were included. The rates for both processes, as well as for other reactions with charged particles, were taken from Cowan et al. (1991).

Code tests for a number of different cases were performed by Panov et al. (2001a), and for a number of explored cases r-process calculations with the same rates gave practically the same isotopic yields as in the paper of Freiburghaus et al. (1999). Network calculations of the α -process with the present code were compared with the results shown by Wittl et al. (1994) and yield rather compatible abundance distributions at the beginning of the r-

Table 1. Parameter values for some of our considered outflows and of relevance for third peak formation.

run	τ_{dyn} [ms]	entropy [k_B/N]	$T_9^{\text{f}}(t_0)$	t_0 [ms]	v_{ini} [km/s]	v_0 [km/s]	$\langle A \rangle$	$\langle Y(A_3)/Y(A_2) \rangle$
1	5	105	1	9	2000	12000	118	10^{-10}
2	2.5	105	1	4.5	4000	24000	127	0.01
3	5	145	1.4	8	2000	10000	128	0.075
4	5	145	0.4	14	2000	33000	128	0.04
5	2.5	145	1	4	4000	20000	144	0.45
6	10	170	1	16	1000	5000	119	10^{-5}
7	5	170	1	8	2000	10000	145	0.75

process, in spite of differences in the employed nuclear reaction rates and the nuclear mass model.

In this context we would like to note that the transition from the α -process to the r-process can only be done correctly on the basis of the same mathematical model. In our calculations we use the same code for both parts of the nucleosynthetic reaction sequence, without artificial deviation into α - and r-process steps.

We compared the seed production as calculated with our full network to results from nuclear statistical equilibrium (NSE) as obtained by Nadyozhin & Yudin (2004), Blinnikov et al. (to be published), and with the NSE-code used by Wittl et al. (1994). We observed rather good agreement at temperatures $T_9 \approx 5$ –6 and a density around $5 \times 10^6 \text{ g cm}^{-3}$. At such temperatures the α -peak is already formed and the mass fraction of seed nuclei (i.e., heavy elements) is still small, the most abundant nuclei in both cases being ^{50}Ti and ^{54}Cr . Small discrepancies between the different calculations emerge mostly from the use of different mass formulas and can lead to smaller differences in the subsequent α - and r-process. They may be important for exact predictions of the abundance flow during the r-processing, but they should not affect the basic results of our investigation.

We also compared our results for the α -process with the calculations made by Wittl et al. (1994), using conditions similar to those of the HT-model of Wittl et al. (1993), i.e., $s = 390$, $Y_e = 0.455$. For an exponential expansion with a timescale of $\tau_{\text{dyn}} = 62 \text{ ms}$, which is the same as in the HT-model, the number density n_n as a function of temperature (Fig. 1, left) is clearly different from what was obtained by Takahashi et al. (1994) (see Fig. 2 therein and the dashed line in the left panel of Fig. 1). When we increase the expansion timescale to $\tau_{\text{dyn}} = 162 \text{ ms}$, our result becomes close to that of Takahashi et al. (1994). The reason for this discrepancy is the fact that our calculations assume homologous expansion with an exponential decrease of density and temperature, whereas the temperature and density in the hydrodynamic model considered by Takahashi et al. asymptote to nonvanishing values, i.e., the temperature approaches $T_9 = 1.5$ during the later expansion. Although r-process elements are formed, neither of our exponential runs leads to the build-up of a strong third r-process peak, despite the high entropy. While in the case with the short expansion timescale ($\tau_{\text{dyn}} = 62 \text{ ms}$) the rapid dilution of the matter prohibits the efficient formation of seed nuclei, the larger expansion timescale ($\tau_{\text{dyn}} = 162 \text{ ms}$) leads to a strong α -process with a lot of seed production and therefore a neutron-to-seed ratio that is too small for the generation of very heavy r-process nuclei. In contrast, Takahashi et al. (1994) obtained a prominent third abundance peak. In their calculation a sufficiently fast initial expansion pre-

vents the formation of too much seed material before the r-process starts, and therefore the neutron-to-seed ratio remains high. The asymptoting temperature and density on the other hand support a high neutron number density for such a long time that neutron capture reactions can assemble nuclei also in the third peak.

For lower entropy, $s = 145$, and higher neutron excess, $Y_e = 0.42$, (Fig. 1, right) the number of free neutrons can also remain large enough to allow for the onset of r-processing when the α -process freezes out at a temperature of $T_9 \sim 2$. In this case, however, much shorter dynamical timescales are needed. Figure 2 displays the decreasing seed formation and increasing neutron-to-seed ratio for smaller expansion timescales τ_{dyn} .

How many neutrons per seed nucleus are needed to form the third abundance peak ($A \sim 196$)? Usually the number mentioned in this context is not less than 150. But this estimate is based on the simple calculation how many neutrons a single ^{56}Fe nucleus must capture to finally, after a chain of beta-decays, end as nucleus in the platinum peak. In the actual r-process, only a fraction of the nuclei that are initially formed by the alpha-process — we call these nuclei the “seed” — will be ultimately transformed to elements and isotopes with the highest mass numbers. Taking into account that the observed ratio of the third to second abundance peak is $Y_{196}/Y_{130} \sim 0.2$, we estimate that the neutron number needed to obtain a sufficiently strong third peak is of the order of $(196 - 60) \times 0.2 \approx 30$. The actual value might even be a bit lower, because the mean atomic number at the freeze-out time of the α -process can be about 80 or more instead of 60 (an exact estimate, however, also depends on the conditions in which the r-processing takes place and the corresponding speed of the abundance flow). Therefore a solar-like formation of the platinum peak can be expected if one has a neutron-to-seed ratio of around 30 *after the freeze-out of charged-particle reactions*.

To judge about the possibility of an r-process for different choices of the parameters of our dynamical model (s , Y_e , τ_{dyn}), we first consider the seed formation and the corresponding time evolution of the neutron-to-seed ratio in the homologous expansion phase. In Fig. 1 we have seen agreement of the free neutron density as a function of time between our calculations and the prior ones by Takahashi et al. (1994) for a suitable choice of the expansion timescale τ_{dyn} (although the heavy-element nucleosynthesis was considerably different as discussed above). Figure 2 shows the neutron-to-seed ratios and the seed abundances, $Y_s = \sum_{Z > 2} Y_Z$, versus temperature for the same cases as displayed in the right panel of Fig. 1. Note that we consider all nuclei with $Z > 2$ as seeds, which is a different definition than used by Terasawa et al. (2001), who restricted seed nu-

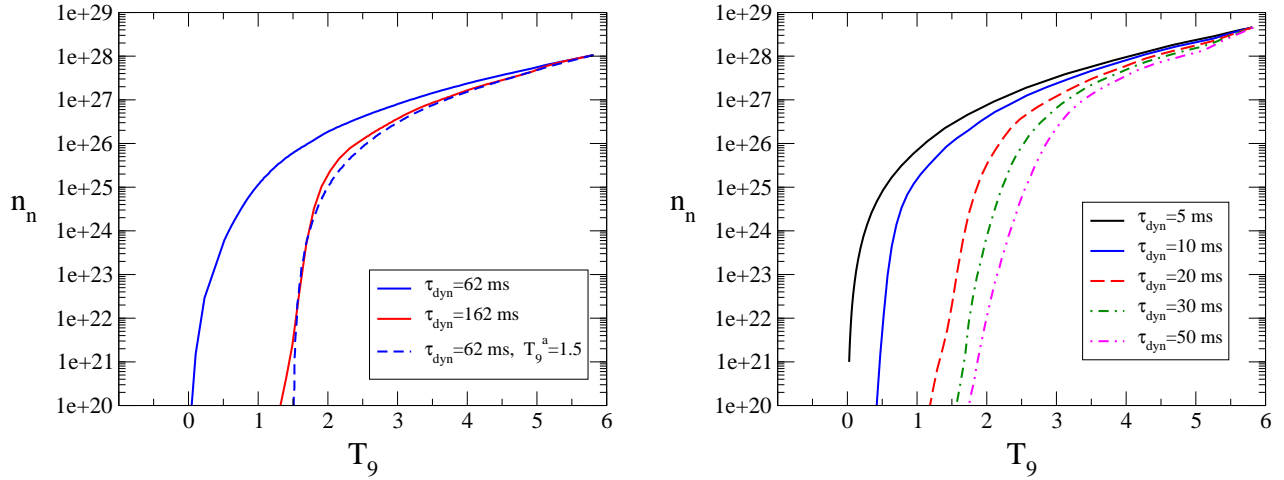


Fig. 1. T_9 -dependence of the free neutron density n_n for $s = 390$ (measured in k_B per nucleon), $Y_e = 0.46$ (left) and $s = 145$, $Y_e = 0.42$ (right). The different curves correspond to different exponential expansion timescales τ_{dyn} as given in the list. The dashed line in the left plot shows the result for conditions close to those in Fig. 7 of Wittl et al. (1994). In the case of the HT-model considered by Wittl et al. (1994), the temperature asymptotes to a value of $T_9^a = 1.5$. The density also decreases so slowly that a high neutron number density is supported long enough for the creation of a strong third r-process peak. In contrast, during the free expansion of very high entropy material with an exponential timescale of 0.62 ms, the matter dilutes too fast to produce large amounts of heavy elements, and no prominent third r-process abundance peak can be formed. In spite of a similar decline of the neutron density with temperature for an expansion timescale of 162 ms, the third abundance peak can also not be assembled in this case, because the slow expansion leads to abundant seed production in a strong α -process and too small a neutron-to-seed ratio.

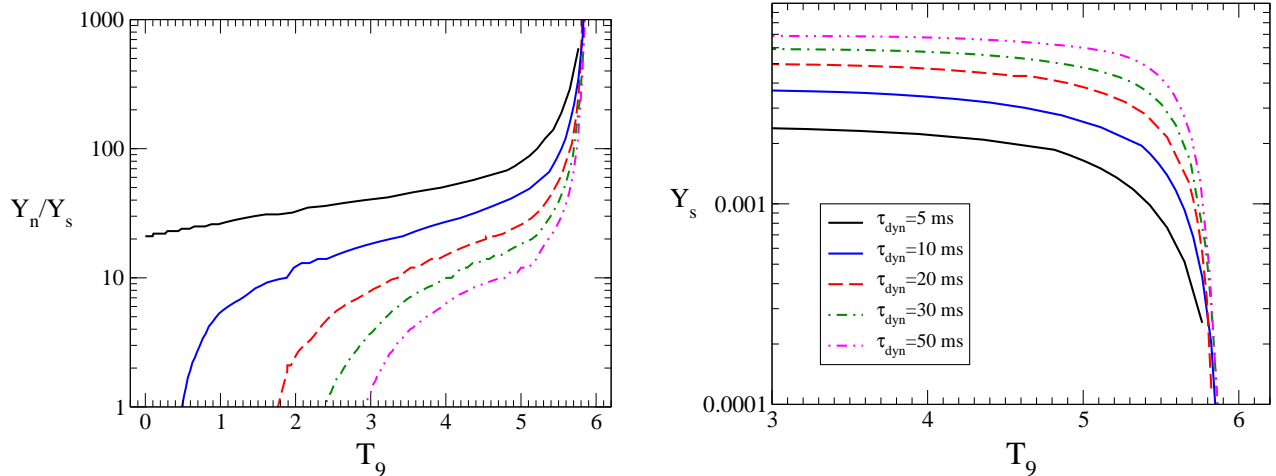


Fig. 2. T_9 -dependence of the neutron-to-seed ratio Y_n/Y_s (left) and of the “seed” number fraction Y_s (right) for an entropy of $s = 145$ and $Y_e = 0.42$. The different curves correspond to different exponential expansion timescales, $\tau_{\text{dyn}} = 5, 10, 20, 30, 50$ ms (the same cases as in the right panel of Fig. 1). At the beginning of r-processing ($T_9 \approx 2$), the free neutron number is sufficiently large to form heavy elements up to the second or even third peak if the dynamical time is less than 10 ms for the considered entropy and electron fraction. For larger values of τ_{dyn} , the free neutrons are exhausted right at the beginning of the r-processing and the number of seed nuclei is too high.

clei to the more narrow range of $70 \leq A \leq 120$ and $Z > 26$. The latter mass range is appropriate when the formation of the second abundance peak in an incomplete r-process is discussed. Here, however, we explore the possibility of third-peak production and consider a combined α - and r-process. In this case the atomic mass number should not be constrained. Because of the very short expansion timescale and the treatment of both the α -process and the r-process within the framework of the same mathematical

model and computer code, a distinction of seed nuclei and r-processed material becomes artificial and one has to carefully judge when this information is measured and what it means for the evolution of the mass number with time. Often it refers to older calculations in which the α - and r-process were computed in two independent steps and with different codes. In this context we note that the amount of heavy nuclei in our calculations is approximately twice as big as found by Terasawa et al. (2002). This difference

is mostly explained by the different model parameters (in particular, Terasawa et al. investigated outflows with higher entropies), but to some extent may also be a consequence of different nuclear rates and included reactions.

With the definition of seed nuclei adopted by us, the seed abundance becomes constant after the freeze-out of the alpha-process and will also be unaffected by the transition to a second stage with modified expansion behavior for the cases considered by us. In contrast, replacing the free (homologous) expansion by a slower second stage of outflow behavior will have an impact on the density of free neutrons as a function of time. The free neutron density determines the r-process path and thus the formation of the heaviest elements in the third abundance peak.

From Fig. 2 (left panel) we see that the expansion timescale for that to happen should be less than about 10 ms. In this case the neutron-to seed ratio Y_n/Y_s as the decisive macroscopic factor for the platinum peak formation reaches the interesting values mentioned above. Naturally, this ratio depends not only on the number of free neutrons, but also on the seed abundance. Figure 2 (right panel) shows that the seed production varies strongly with the expansion timescale: if the dynamical time is large, a lot of seed is assembled and all neutrons will be captured faster than the platinum peak begins to appear. With shorter expansion timescale the seed production drops and at the same time the density of free neutrons increases (see right panel of Fig. 1). The consequence of both trends with reduced τ_{dyn} is a strong growth of the Y_n/Y_s ratio that is present at the beginning of the r-process.

However, as already discussed above in the context of Fig. 1, too rapid expansion can also be disadvantageous for a strong r-process. When the dynamical timescale becomes very short, the expansion and gas dilution proceed faster than the rate of recombination of alpha particles to seed nuclei and subsequently the rate of neutron captures. For the conditions considered in Fig. 2 this happens when the seed abundance drops significantly below a critical value of about $Y_A \sim 3 \times 10^{-3}$. The homologous expansion is then so rapid that no strong 3rd peak forms, despite a very high neutron-to-seed ratio after the freeze-out of charged-particle processes.

Of course, as discussed in detail in many previous works, besides the expansion timescale, the entropy and the neutron excess (or Y_e), have a sensitive influence on the strength of the r-processing, i.e., on the question how many nuclei with mass numbers above the second abundance peak and in particular near the third peak can be formed. In any case, for rapid expansion (small τ_{dyn}) the seed production is reduced and the neutron-to-seed ratio becomes more favorable for a strong r-process. The heavier the seed nuclei at the end of the α -process are, the lower can be the required number of free neutrons be. This was already discussed by, e.g., Panov & Chechetkin (2002), who showed that fairly low neutron/seed ratios are already sufficient when the seed material at the freeze-out time of charged-particle reactions consists mostly of nuclei in the second abundance peak.

3. Asymptotic behavior of temperature and density and formation of the platinum peak

Our combined (α +r)-code was applied to nucleosynthesis calculations assuming the two-stage expansion behav-

ior described above, with a second phase of either constant or slowly decreasing temperature and density following a first phase of rapid, exponential expansion. Our calculations were started at a temperature of $T_9 = 6$, assuming NSE at this point. For conditions similar to those given in Fig. 2 of Terasawa et al. (2001) with a short expansion timescale of $\tau_{\text{dyn}} = 5$ ms, we obtained basically the same results for the development of the neutron number density and average neutron separation energy until about half a second, and found gross agreement of the structure of the abundance distribution. Smaller discrepancies might be attributed to differences in the initial composition and nuclear reaction rates. The number fraction of seed nuclei reported by Terasawa et al. (2001), $Y_s \sim 0.001$, is a bit low compared to our results, but this is probably mainly caused by a different definition of “seeds”.

In contrast, we were not able to confirm the formation of the third abundance peak for conditions similar to those considered by Terasawa et al. (2002) with an assumed expansion timescale of $\tau_{\text{dyn}} = 25$ ms. Besides not providing exact information about the initial density and the kind of network used for the alpha- and r-process calculations (a full network or off-line calculations for the r-processing?), some of the results and explanations are hard to reproduce in detail. For example, the calculations done by us with different NSE codes (including that of Nadyozhin and Yudin 2004) and also the simulations by Wittl et al. (1994) show that α -particles reassemble mainly down to temperatures around $T_9 = 5$ –6, somewhat dependent on the density, but not at temperatures as low as $T_9 = 4$ (see Fig. 1 in Terasawa et al. 2002). Moreover, they argued that a lower value of the asymptotic temperature is favorable for a successful r-processing by allowing for a higher neutron-to-seed ratio, because such a lower “outer boundary” temperature reduces charged-particle reactions and thus the production of seed nuclei. This suggested influence of the chosen asymptotic temperatures in the range between $T_9 = 0.4$ and $T_9 = 1.3$, however, is implausible, because charged-particle reactions become inefficient already at temperatures of $T_9 \approx 2$, when the thermal energies of protons and α -particles become too low for enabling these particles to overcome the nuclear Coulomb barriers.

We will therefore not further attempt to compare our calculations with those done by Terasawa et al. (2002). Instead, we will in the following present our results for the formation of the third abundance peak in dependence of entropy, electron fraction, and dynamical timescale during the first, exponential expansion phase. In particular we will also study variations with the asymptotic values of temperature and density during the second, slower phase of expansion. This will help us in the analysis of the physical effects that can explain our results. Our goal is to develop a deeper understanding of the influence of the late-time behavior of neutrino-driven winds on the possibility of strong r-processing in such an environment.

To this end we carried out a set of calculations for exponential timescales in the range from 1.0 to 25 ms and for four values of the wind entropy (in units of Boltzmann’s constant per nucleon), $s = 105, 145, 170$, and 200. The initial neutron to proton ratio was determined by an electron fraction of usually $Y_e = 0.42$; some runs were performed with a value of $Y_e = 0.46$.

Our special attention was on the second stage of slower expansion, which was chosen to either proceed with con-

stant temperature and density (Eqs. 3–6) or gradually decreasing temperature and density (Eqs. 7–10). In the former case we defined the asymptotic temperature as $T_9^f(t \geq t_0) \equiv T_9^0 = \text{const}$ (Sect. 3.1), in the latter case the temperature was assumed to follow a power-law time-dependence according to $T_9^f(t) \equiv T_9^f(t_0) \times (t_0/t)^{2/3}$ for $t \geq t_0$ (Sect. 3.2). The range of temperatures $T_9^f(t_0)$, where the second expansion phase began, had a broad overlap with the “boundary temperatures” considered by Terasawa et al. (2001, 2002) and Wanaajo et al. (2002).

Our standard calculations were performed with an entropy of $s = 145$. Values of less than $s \approx 100$ turned out to lead only to the production of the second abundance peak around $A \sim 130$, but r-processing up to the platinum peak was not possible when the other characteristic wind parameters were varied within the limits mentioned above.

3.1. Constant asymptotic temperature and density

In this section we consider an exponential first expansion phase that is superseded at evolution time t_0 by a second, slow expansion phase whose asymptotic velocity at large radii goes to zero. In this case the density and temperature during the second phase adopt constant values (Eqs. 3–6). We explore various choices of the asymptotic temperature $T_9^f(t \geq t_0) \equiv T_9^0 = \text{const}$ between 0.1 and 1.4. For an entropy of $s = 145$, for which results are displayed in Figs. 3–5, these temperatures correspond to constant densities ρ_0 between about 1 g cm^{-3} and 10^4 g cm^{-3} . For these values the neutron number density at time t_0 shows differences by more than three orders of magnitude (see Fig. 3). Although the lowest assumed value of $T_9^0 = 0.1$ might appear extreme, because it requires very rapid exponential expansion for a longer time with fairly high velocities at the end of this phase, the wide range of asymptotic temperatures allows us to better understand the dependence of the nucleosynthesis on the late-time expansion behavior of the outflowing matter.

When the asymptotic temperature is as high as $T_9^0 \approx 1.4$, the third peak hardly develops (see the abundance distribution at the end of our calculations in the right panel of Fig. 3). Only when the asymptotic temperature is reduced from this value to smaller numbers, the platinum peak grows in strength, because the free neutrons are exhausted more rapidly and the r-processing proceeds faster towards the high mass-number region. The latter fact can be seen by comparing the decrease of the neutron density with time for $T_9^0 = 1.4, 1,$ and 0.4 in the left panel of Fig. 3, and it is also visible from the neutron-to-seed ratios Y_n/Y_s as functions of time in the left panel of Fig. 4. When the asymptotic temperature is lowered to less than $T_9^0 \approx 0.3$, the free neutron density n_n during the slow-expansion phase becomes so low that the formation of the third abundance peak under such conditions slows down considerably. Correspondingly, n_n as well as Y_n/Y_s decrease less quickly (see again the left panels of Figs. 3 and 4) and the height of the third peak at the time of neutron exhaustion becomes clearly lower (Fig. 3, right panel).

This inversion of the third peak formation with decreasing value of the asymptotic temperature T_9^0 can be clearly seen from the time evolution of the average of the yields in the platinum peak relative to those in the $N = 82$ peak, $\langle Y(A_3)/Y(A_2) \rangle$, in the right panel of Fig. 4. The displayed quantity is defined by summing up the produced yields for

five mass numbers around $A = 130$ and $A = 196$ and then computing the ratio²

$$\left\langle \frac{Y(A_3)}{Y(A_2)} \right\rangle \equiv \frac{\sum_{193}^{197} Y(A_i)}{\sum_{128}^{132} Y(A_i)}. \quad (11)$$

The left panel of Fig. 5 shows the sensitivity of the final value of this ratio to the chosen temperature $T_9^f(t > t_0) = T_9^0$. While the growing strength of the platinum peak with lower asymptotic temperature agrees with the finding by Terasawa et al. (2002), their conclusion of a more efficient r-processing for lower “outer boundary pressure/temperature” obviously does not hold any more when this temperature is less than $T_9 \approx 0.3$, which is below the range explored by them.

We note here that often the change of the average atomic number is used for following the build-up of heavy elements beyond the $A \approx 130$ abundance peak. We found this quantity to be less suitable for this purpose than our height ratio $\langle Y(A_3)/Y(A_2) \rangle$, in particular when the second peak is much stronger than the third. A growth of the latter by one order of magnitude can mean a change of $\langle A \rangle$ by just one or a few units, whereas $\langle Y(A_3)/Y(A_2) \rangle$ varies sensitively and thus serves well as a tracer of changes of the abundance distribution in the high-mass number region.

The variation of the strength of the third peak with different asymptotic temperatures can be understood from the sensitivity of the neutron capture rates and nuclear photodisintegration rates to the neutron number density and temperature, respectively, and by the competition of these rates. This competition determines the location of the r-process path and thus the speed of the nucleosynthesis, which is defined by the β -decay rates. When the temperature during the second, slow expansion phase is large ($T_9 \gtrsim 1.0$), the (γ, n) -reactions are very fast and the r-process path lies close to the stability region. The r-process flow beyond the second peak is then rather weak because of the low beta-decay rates and a correspondingly slow progression of the nuclear flow. When the asymptotic temperature is reduced to $T_9^0 \approx 0.2$ – 0.7 , the (γ, n) -rates decrease and the r-process path moves towards the neutron-drip line where the β -decay rates are higher. Therefore the r-processing proceeds faster beyond the second peak, leading to a more rapid drop of the free neutron density and a more efficient third peak production. When the asymptotic temperature is lowered to less than $T_9^0 \approx 0.2$ during the late expansion phase, the neutron densities are very low so that the r-process path returns to a location closer to the β -stable region. In this case the β -decays again become slower and therefore the r-process nucleosynthesis decelerates and the third peak builds up to a smaller height.

These movements of the r-process path are a consequence of the different influence of a change of the asymptotic temperature on the (γ, n) - and the neutron captures rates. For asymptotic temperatures in the interval $0.2 \lesssim T_9^0 \lesssim 1.0$ the (γ, n) -rates are very sensitive to temperature variations. In contrast, the neutron capture rates change with the corresponding variations of the density and free neutron density less strongly. A reduced temperature therefore decreases the photodisintegration rates significantly, whereas the neutron captures remain fast despite the lower

² A similar peak ratio was considered in a recent paper by Beun et al. (2008).

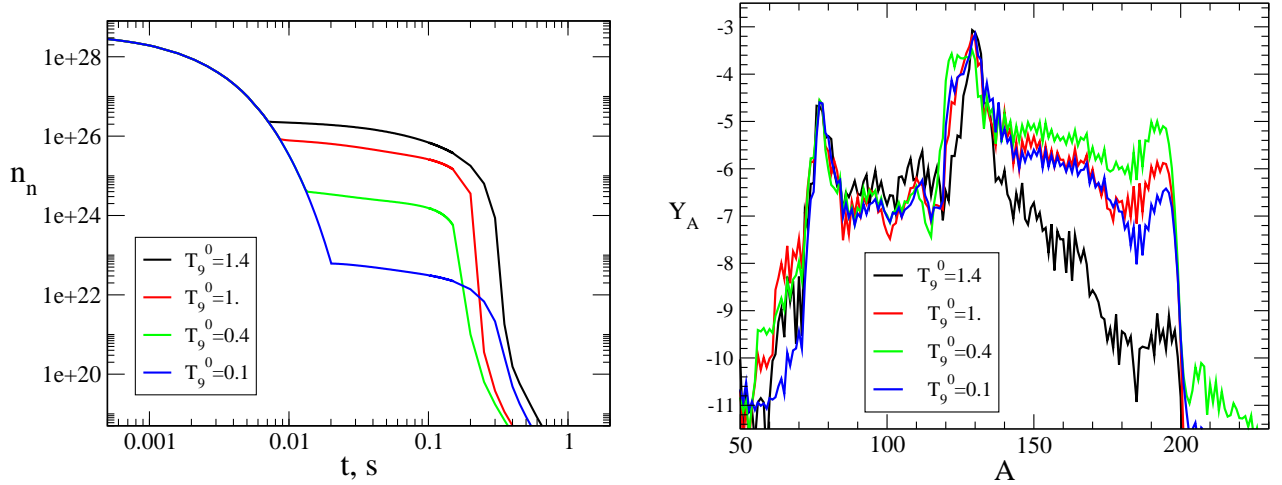


Fig. 3. Time dependence of the neutron number density, $n_n(t)$ (left), and the final abundance distributions, Y_A , resulting from our network calculations for $s = 145$, $Y_e = 0.42$, a short dynamical timescale of $\tau_{\text{dyn}} = 5$ ms, and different values of the constant asymptotic temperature $T_9^f(t \geq t_0) = T_9^0(t_0)$ during the second stage of the ejecta expansion. The corresponding values of T_9^0 are listed in the inset.

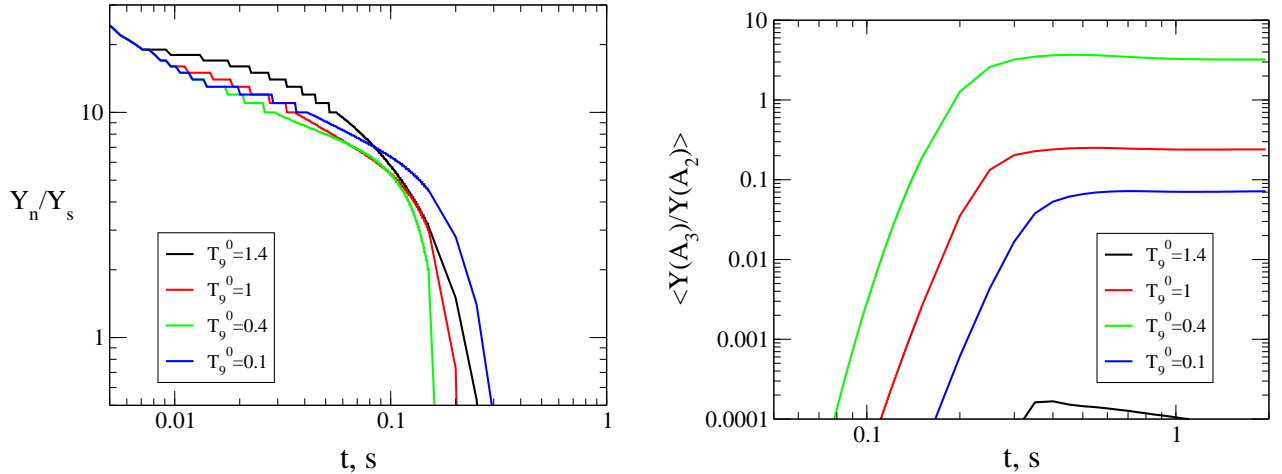


Fig. 4. Time dependence of the neutron-to-seed ratios, Y_n/Y_s (left), and of the height of the third abundance peak relative to the second, $\langle Y(A_3)/Y(A_2) \rangle$ (right, in percent) for the same conditions as in Fig. 3 ($s = 145$, $Y_e = 0.42$, $\tau_{\text{dyn}} = 5$ ms, $T_9^0 = \text{const}$ as given in the inset). The inversion of the third peak formation with decreasing asymptotic temperature can be clearly seen: when T_9^0 is lowered from 1.4 to 0.4, the ratio of the third peak to the second increases, and when T_9^0 is reduced even further, $\langle Y(A_3)/Y(A_2) \rangle$ begins to drop again.

neutron density. When $T_9^0 \lesssim 0.2$, the (γ, n) -rates become less relevant, but neutron captures still compete with β -decays. For such low temperatures and thus low neutron densities, the neutron capture rates are too small to drive the r-process path far away from the valley of stability.

The shift of the r-process path that is caused by different asymptotic temperatures (and connected parameters) manifests itself in different isotopic profiles of the elements formed by the r-processing (i.e. in different yield of the isotopes of an element). This can be seen for the case of cadmium in the right panel of Fig. 5.

3.2. Power-law time-dependence of the asymptotic temperature and density

In this section we consider the case that the initial exponential phase is superseded at time $t = t_0$ by a slow expansion phase in which the temperature and density decay according to power laws, i.e., $T_9^f(t) \propto T_9^f(t_0)/t^{2/3}$ and $\rho^f(t) \propto \rho^f(t_0)/t^2$ for $t \geq t_0$ (Eqs. 7–10).

For our standard set of wind parameters, $s = 145$ (in units of Boltzmann's constant per nucleon), $Y_e = 0.42$, and $\tau_{\text{dyn}} = 5$ ms already used in Sect. 3.1, Fig. 6 shows the time evolution of the free neutron density (left panel) and the final abundance distributions for four different values of the transition temperature $T_9^f(t_0)$ (right panel). The formation of the third abundance peak turns out to be fairly insensitive to variations of $T_9^f(t_0)$ between about 0.4 and 1.4.

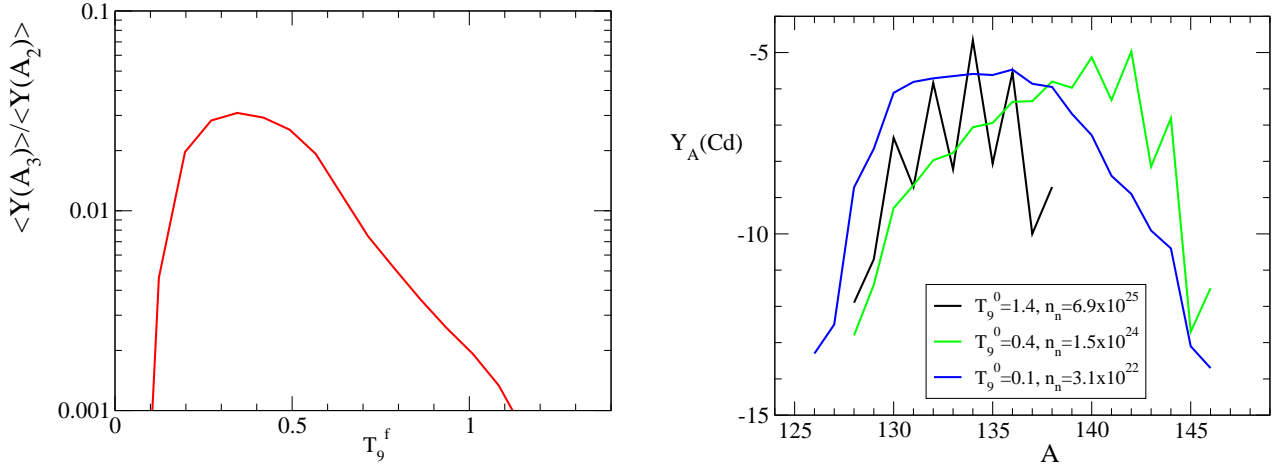


Fig. 5. *Left:* The changing strength of the third abundance peak, measured in terms of the ratio $\langle Y(A_3)/Y(A_2) \rangle$, as function of the asymptotic temperature $T_9^f(t > t_0) = T_9^0$ for the conditions considered in Fig. 3 ($s = 145$, $Y_e = 0.42$, $\tau_{\text{dyn}} = 5$ ms, $T_9^0 = \text{const}$). The relative height of the third abundance peak depends strongly on the value of T_9^0 because of a sensitive influence of this temperature on the r-process path. This can be seen in the distribution of cadmium isotopes at an evolution time of $t = 0.1$ s for three different cases of the asymptotic temperature (*right*; the neutron number densities in the inset are those at $t = 0.1$ s in Fig. 3). When T_9^0 is lowered from 1.4 to 0.4, the free neutron density and thus the neutron capture rate in the slow, second phase of the expansion decreases less strongly than the (γ, n) -rates, which are extremely sensitive to the temperature. As a consequence, the r-process path is shifted towards the neutron-drip line (compare the isotope distribution given by the green line) where the β -decay rates are higher and the r-processing proceeds so rapidly that there is time to form a strong third abundance peak. For even lower asymptotic temperature the (γ, n) -rates do not play an important role and the strength of the r-processing is determined by the free neutron density and the β -decay rates. Since the r-process path returns again to a location closer to the valley of stability (see the isotope distribution of the blue line), the β -decay rates are lower and the nucleosynthesis slows down. Therefore a strong third peak cannot be formed.

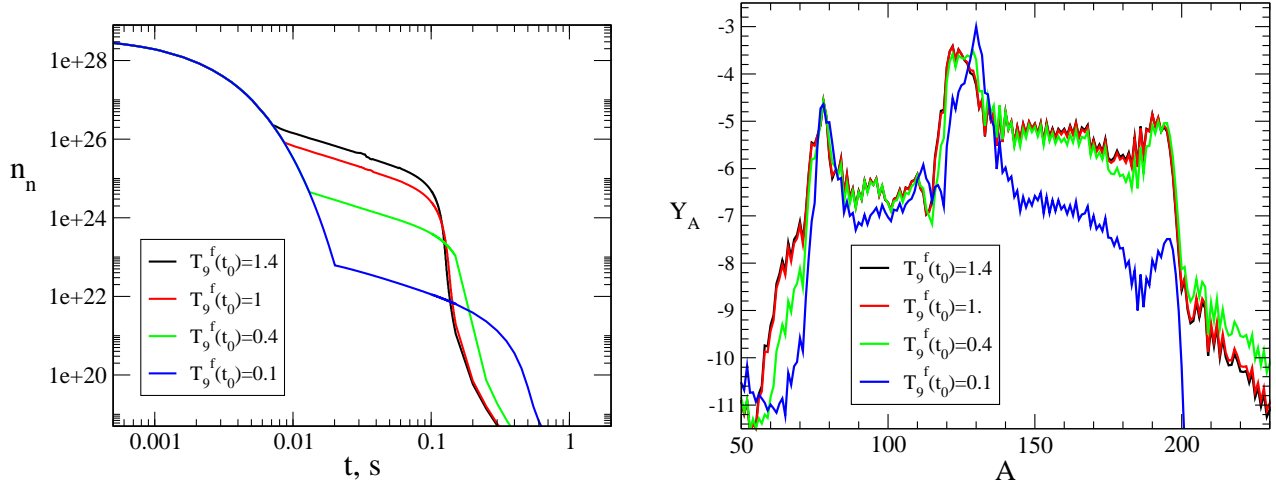


Fig. 6. Same as Fig. 3 (with $s = 145$, $Y_e = 0.42$, and an exponential timescale $\tau_{\text{dyn}} = 5$ ms), but for a power-law decay of the temperature during the second, slow expansion phase: $T_9^f(t) \propto T_9^f(t_0)/t^{2/3}$ for $t \geq t_0$. The left plot shows the time dependence of the neutron number density, $n_n(t)$, the right plot the corresponding final abundance distribution for different values of the transition temperature $T_9^f(t_0)$ as given in the inset. Different from the case with constant asymptotic temperature in Fig. 3, the temperature and thus the photodisintegration rates drop rapidly also in the slow expansion phase. Neutron captures are therefore able to produce a prominent third abundance peak even for the largest considered value of the transition temperature, $T_9^f(t_0) = 1.4$. The height of the third peak relative to the second is very similar in the whole range of temperatures $T_9^f(t_0)$ between 0.4 and 1.4, and the inversion behavior of $\langle Y(A_3)/Y(A_2) \rangle$ with $T_9^f(t_0)$ is absent.

For all transition temperatures in this interval a prominent third peak appears.

Since the temperature in the post-exponential phase drops rapidly, the strongly temperature-dependent (γ, n) -

reactions become unimportant very soon, while the considered entropy allows a high free neutron density ($n_n \geq 10^{22}$) to be present still for a long time. At such conditions the r-process path moves very close to the neutron-drip line and returns to the classical r-process path during free neutron exhaustion (Panov 2003). For the considered conditions its location shifts significantly only when the free neutron density changes by 2–3 orders of magnitude. This explains the relative robustness of the abundance yields to variations of $T_9^f(t_0)$ around 1.0.

The left panel of Fig. 7 displays the evolution of the neutron-to-seed ratios Y_n/Y_{seed} that correspond to the neutron number densities of Fig. 6. With an entropy of $s = 145$ and an exponential timescale $\tau_{\text{dyn}} = 5$ ms the values of Y_n/Y_{seed} at the time when the r-process has made the second abundance peak (at $t \approx t_0$) are around 20 for $T_9^f(t_0) = 0.4$ –1.4. As discussed in Sect. 2, this is a slightly insufficient number of neutrons per seed nucleus to create a third peak with exactly the observed yields. The small underabundance of the third peak can also be seen in the right panel of Fig. 7, where the height of the platinum peak relative to the tellurium peak is given as function of time. Different from the case of constant asymptotic temperature (see Fig. 4), $\langle Y(A_3)/Y(A_2) \rangle$ is nearly the same for $T_9^f(t_0) = 1.0$ and 1.4, and is only slightly reduced for $T_9^f(t_0) = 0.4$. For even lower transition temperatures the height of the third peak drops steeply. This is evident from the blue line in the left panel of Fig. 8 and is a consequence of a significantly smaller neutron-to-seed ratio at $t = t_0$.

The left panel of Fig. 8 provides a direct comparison of the variation of $\langle Y(A_3)/Y(A_2) \rangle$ with the transition temperature between the exponential first expansion phase to the second phase of either constant temperature or power-law temperature decrease. Above a transition temperature $T_9^f(t_0) \sim 0.4$ the behavior in both cases is dramatically different. While in the case of constant asymptotic temperature the relative height of the third peak decreases with higher values of T_9^0 (see Fig. 5 and Sect. 3.1), a power-law decay of the temperature in the second expansion phase leads to a prominent platinum peak for all values of $T_9^f(t_0)$ between 0.5 and 1.4. The reason is again the large sensitivity of the photodisintegration reactions to the late-time behavior of the temperature. Due to the power-law decline the temperature drops within milliseconds to values where a (n,γ) - (γ,n) equilibrium is no longer possible but is replaced by a quasi-equilibrium between (n,γ) -reactions and β -decays. The nucleosynthesis at these conditions resembles the n-process of Blake & Schramm (1976), but there it was discussed to occur because of a decrease of the neutron density below 10^{18} , while here it happens because of a decrease of the temperature and an associated strong reduction of the (γ,n) -rates. It should be noted that the prominent odd-even effect in the isotope distributions in the right panel of Fig. 5 for $T_9^0 = 1.4$ and 0.4 has practically disappeared in Fig. 8, where the isotope distributions for the same values of the transition temperature are much smoother.

We point out here that the r-processing of heavy nuclei through a quasi-equilibrium of (n,γ) -reactions and β -decays at conditions where photodisintegrations are practically unimportant was recently also discussed³ by Wanajo

(2007), who coined the term “cold r-process”. We prefer to call it “r β -process”, because this name is conform with the denotation of other processes (r-process, rp-process, ν p-process,...) and reflects the essential aspect that characterizes this variant of the rapid neutron-capture process.

3.3. Variations of wind parameters in the exponential phase

In this section we will discuss the sensitivity of our nucleosynthesis results to variations of the characteristic outflow conditions like exponential expansion timescale, entropy, and electron fraction. Table 1 lists corresponding parameter values for some of the considered outflows: τ_{dyn} is the exponential expansion timescale⁴, $T_9^f(t_0)$ and t_0 the temperature and time at which the transition occurs from the exponential first expansion phase to the second phase with power-law decline of temperature and density, $v_{\text{ini}} = R_{\text{ini}}/\tau_{\text{dyn}}$ is the initial outflow velocity at an assumed initial radius $R_{\text{ini}} = 10$ km, $v_0 = v_{\text{ini}} \exp(t_0/\tau_{\text{dyn}})$ is the outflow velocity at transition time t_0 , $\langle A \rangle$ is the average mass number of nucleosynthesis yields, and $\langle Y(A_3)/Y(A_2) \rangle$ the ratio of the height of the third abundance peak relative to the second as defined in Sect. 3.1.

As discussed in Sect. 2, the strength of the r-process is determined by the abundance of seed nuclei that is able to form, and by the number of remaining free neutrons when the r-processing sets in at $T_9 \approx 2$ –3. For the homologous outflows considered there we saw that a larger dynamical timescale increases the efficiency of seed formation at the expense of free neutrons, and for a very short dynamical timescale the expansion can be so rapid that α particles and neutrons do not have any time to assemble to very heavy elements. In both cases a strong third abundance peak cannot develop. A smaller value of the outflow entropy also allows neutrons, protons, and α -particles to recombine to nuclei more efficiently and therefore lower entropies have a similar effect as a slow expansion.

For a given value of the entropy, significant production of high-mass elements therefore on the one hand requires that the expansion timescale is sufficiently long, corresponding to a critical lower limit Y_s^{cr} of the seed abundance at the start of the r-processing. On the other hand, the expansion must be enough fast because otherwise the seed production exceeds Y_s^{cr} too much, and the platinum peak cannot be formed because of a unfavorably low neutron-to-seed ratio. Our systematic runs for homologous outflows showed (see Fig. 2) that with an entropy of $s = 145$ and an electron fraction of $Y_e = 0.42$ only exponential timescales

however, shares some basic features with the simple two-stage expansion behavior considered in our work, even in the absence of a decelerating wind termination shock. Neutrino-driven winds show an approximately homologous expansion (i.e., $v \propto r$) and thus a nearly exponential increase of the radius and velocity with time only up to some distance, but then the velocity continues to grow less rapidly. This is not dissimilar to the transition from a first exponential stage to a second phase of less rapid expansion in our approach.

⁴ We stress that comparing our expansion timescale with those given in other papers requires some caution. Sumiyoshi et al. (2000) and Terasawa et al. (2002) defined the expansion timescale as e-folding time at $T = 0.5$ MeV, which is compatible with our use. In contrast, Wanajo et al. (2001, 2002) defined it as the cooling time from $T = 0.5$ MeV to $T = 0.2$ MeV, which is about 10% smaller.

³ Different from us, Wanajo (2007) used neutrino-driven wind trajectories obtained as solutions of the steady-state wind equations. Such a more realistic description of the outflow dynamics,

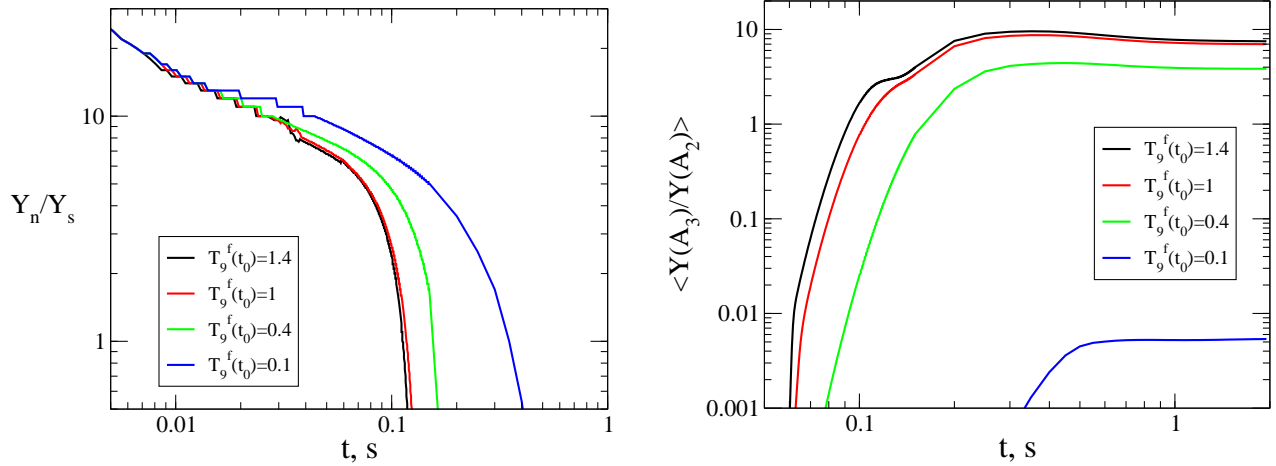


Fig. 7. Same as Fig. 4 (with $s = 145$, $Y_e = 0.42$, and an exponential timescale $\tau_{\text{dyn}} = 5$ ms), but for a power-law decay of the temperature during the second, slow expansion phase: $T_9^f(t) \propto T_9^f(t_0)/t^{2/3}$ for $t \geq t_0$. The left plot shows the time-dependent neutron-to-seed ratio Y_n/Y_s , the right plot the height of the third abundance peak relative to the second ($\langle Y(A_3)/Y(A_2) \rangle$, in percent) as functions of time. The weak dependence of the r-processing on variations of the transition temperature $T_9^f(t_0)$ between 0.4 and 1.4 as visible in the right panel of Fig. 6 is also evident from these two plots.

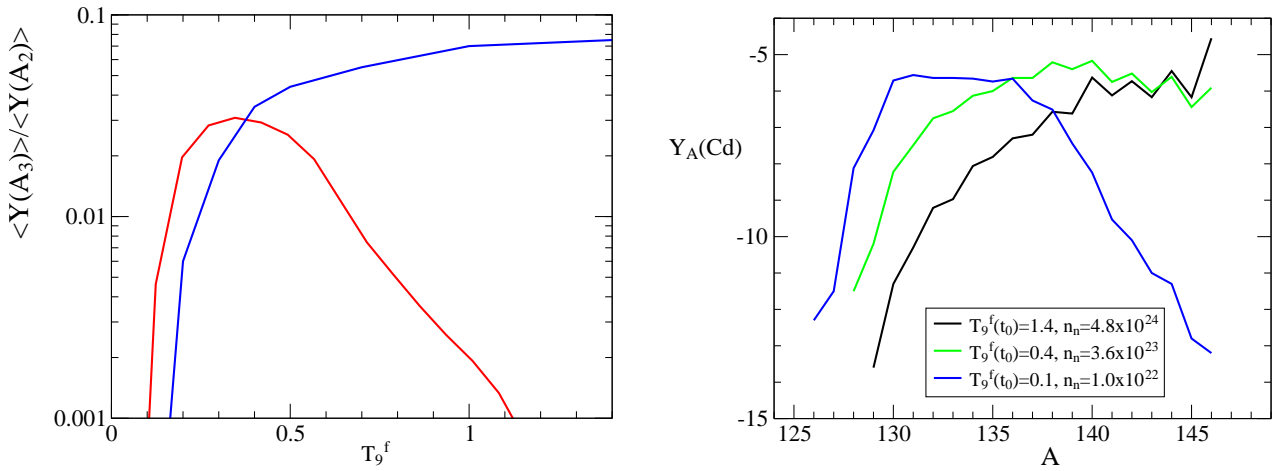


Fig. 8. *Left:* Height of the third abundance peak relative to the second, measured in terms of the ratio $\langle Y(A_3)/Y(A_2) \rangle$, as function of the temperature $T_9^f(t_0)$ for a power-law decay of the temperature during the second, slow expansion phase (blue curve) compared to the dependence of this quantity on $T_9^f(t > t_0) = T_9^0$ in the case of constant asymptotic temperature (red line, see also left panel of Fig. 5). The other wind parameters are again the same as in Figs. 3–7 ($s = 145$, $Y_e = 0.42$, $\tau_{\text{dyn}} = 5$ ms). The right panel shows the distribution of cadmium isotopes at time $t = 0.1$ s for the values of $T_9^f(t_0)$ listed in the inset; the neutron number densities at $t = 0.1$ s are given, too (cf. Fig. 6). The plot should be compared with the right panel of Fig. 5.

τ_{dyn} of less than about 10 ms lead to a neutron number fraction of $Y_n \gtrsim 0.05$ and thus to neutron-to-seed ratios around 20 at the beginning of the r-process. Only then the nuclear flow has a chance to go beyond a mass number of 130 and to reach the range of $A \sim 196$, although the third peak may still be significantly underabundant compared to solar values (see below). The critical limit for the seed abundance turned out to be $Y_s^{\text{cr}} \sim 0.003$ (cf. Sect. 2). Of course, this number depends on s and Y_e , and the homologous expansion timescale that enables third peak formation is shorter for lower entropy values.

Let us now discuss the case in which the homologous outflow with its exponential density and temperature decline is replaced by a slower power-law temperature decay

during the late expansion stage, i.e. after the freeze-out of charged-particle reactions. This makes strong r-processing up to the platinum peak possible for a much wider range of dynamical timescales τ_{dyn} than in the case of purely homologous evolution, practically for all values below some upper limit. This can be seen in Fig. 9, which displays the time-evolution of the neutron number density and the final abundance distribution for different choices of entropies and dynamical timescales. The second stage of power-law temperature decline is assumed to set in at $t = t_0$ with a transition temperature of $T_9^f(t_0) = 1$. A pronounced platinum peak develops for $s = 105$ if $\tau_{\text{dyn}} \lesssim 2.5$ ms, for $s = 145$ this needs $\tau_{\text{dyn}} \lesssim 5$ ms, and for $s \approx 170$ –200 it requires $\tau_{\text{dyn}} \lesssim 10$ ms. An extreme case with $s = 200$ and $\tau_{\text{dyn}} = 1$ ms leads to

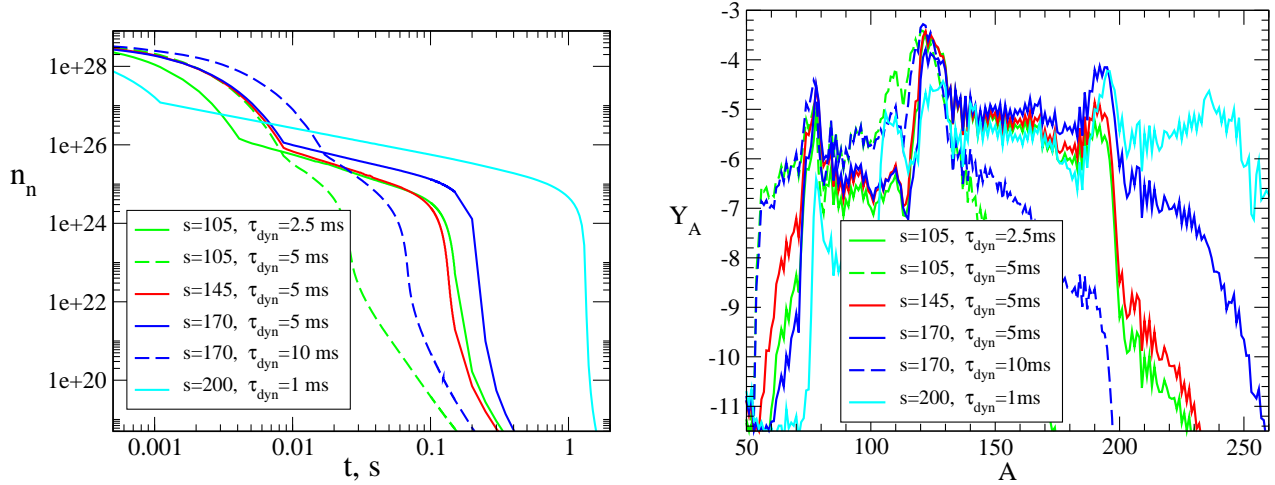


Fig. 9. Time evolution of the free neutron density (*left*) and final abundance distributions of r-process nuclei (*right*) for outflows with different assumed entropies s and exponential expansion timescales τ_{dyn} as listed in the inset. Different entropy values are associated with different line colors, a variation of the expansion timescale with dashed lines. In all cases we assumed $Y_e = 0.42$ and a transition temperature of $T_9^f(t_0) = 1$ between the exponential first expansion phase and the second phase of power-law temperature decline. The cyan line corresponds to the most extreme considered case with an entropy of $s = 200$ and a dynamical timescale of $\tau_{\text{dyn}} = 1$ ms. It serves for demonstrating the influence of fission cycling (see also Fig. 11).

fission cycling and demonstrates that even for very fast homologous expansion during the first stage the slower evolution in the second phase allows all neutrons to be captured into heavy nuclei. The dashed lines belong to cases where the expansion in the homologous phase is too slow for third peak formation.

Figure 9 demonstrates that for a wide range of timescale-entropy combinations in the considered intervals, $2.5 \text{ ms} \lesssim \tau_{\text{dyn}} \lesssim 10 \text{ ms}$ and $100 \lesssim s \lesssim 200$, heavy r-process elements up to the third abundance peak and beyond can be produced. Inspecting our results we find that a very strong platinum peak appears for conditions that roughly fulfill the relation $s \gtrsim 10(\tau_{\text{dyn}} + 10)$.

In Fig. 10 the sensitivity of the r-processing to variations of Y_e is shown in the case with $s = 170$ and $\tau_{\text{dyn}} = 5$ ms. In the left panel one can see that a change of Y_e from 0.42 to 0.46 leads to a reduction of n_n at the beginning of the r-process and a more rapid exhaustion of free neutrons. The yields beyond the second peak are correspondingly lower, with a growing discrepancy at higher mass numbers A (right panel of Fig. 10). While for $Y_e = 0.42$ the platinum peak is slightly overabundant compared to observations (see below), increasing Y_e by about 10% to 0.46 is enough to lead to a significant underproduction. For the considered short dynamical timescale this can be compensated by a roughly 30% higher value of the outflow entropy.

In Fig. 11 we provide an overview of the platinum peak formation in dependence of the entropy and dynamical timescale of the model outflows, using $Y_e = 0.42$ and assuming a transition temperature of $T_9^f(t_0) = 1$ between the exponential first cooling phase and the second phase with power-law decrease of temperature and density. The left panel confirms what we described above: for higher values of the entropy the $A \sim 196$ peak can be assembled for an increasingly wider range of expansion timescales. The bold horizontal lines in the left panel mark the observational band for the abundance ratio $\langle Y(A_3)/Y(A_2) \rangle$. The

third peak relative to the second tends to become overabundant compared to the observations when the expansion timescale is low, whereas it remains too weak for long expansion timescales.

The dashed line in the left panel of Fig. 11 corresponds to runs with $s = 145$ where a constant density and temperature were adopted during the second phase instead of the power-law behavior. The differences between the dashed and solid lines for the same entropy are large, in particular for longer dynamical timescales. This demonstrates again the importance of the late-time behavior of the outflow. This importance, however, is significantly reduced when the transition temperature $T_9^f(t_0)$ is chosen to be near 0.4 (see the left panel of Fig. 8).

For entropies near 200 or higher fission cycling can occur. The right panel of Fig. 11 shows the time evolution of the second and third abundance peaks and of the ratio between both for a case with $s = 200$, $\tau_{\text{dyn}} = 1$ ms, and $Y_e = 0.42$. The periodic changes of the abundances and of $\langle Y(A_3)/Y(A_2) \rangle$ reflect the repeated propagation of nucleosynthesis wave through the transuranium region via fission cycling (the number of nuclear species is increased roughly by a factor of three due to fission), similar to what was observed by Panov et al. (2003), Goriely et al. (2005), and Beun et al. (2008). The overabundance of the platinum peak in this case depends significantly on the nuclear data (Panov et al. 2001b) and should be explored separately on the basis of new fission data calculations (Panov et al. 2005).

4. Discussion and conclusions

Focussing on the high-entropy neutrino-driven wind environment, we investigated the sensitivity of r-process nucleosynthesis to the asymptotic low-temperature behavior that is assumed to follow an approximately homologous expansion when the wind outflow is decelerated at collid-

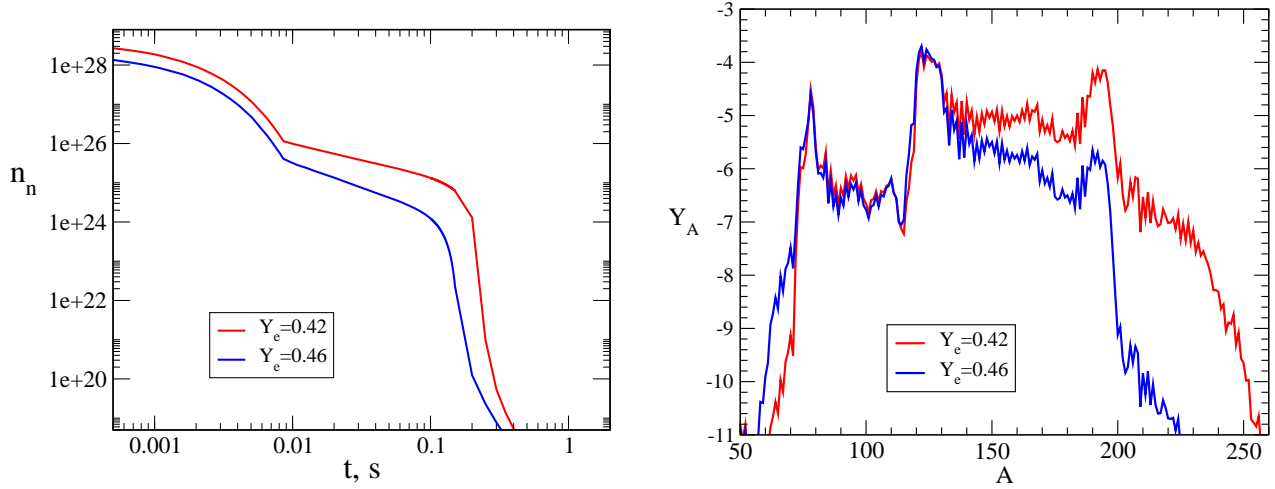


Fig. 10. Time-evolution of the free neutron number density (*left*) and final abundance distribution of r-process nuclei (*right*) for $Y_e = 0.42$ (red lines) compared to $Y_e = 0.46$ (blue lines). In both cases we used $s = 170$, $\tau_{\text{dyn}} = 5$ ms, and a transition temperature of $T_9^f(t_0) = 1$ between the exponential first expansion phase and the second phase of power-law temperature decline.

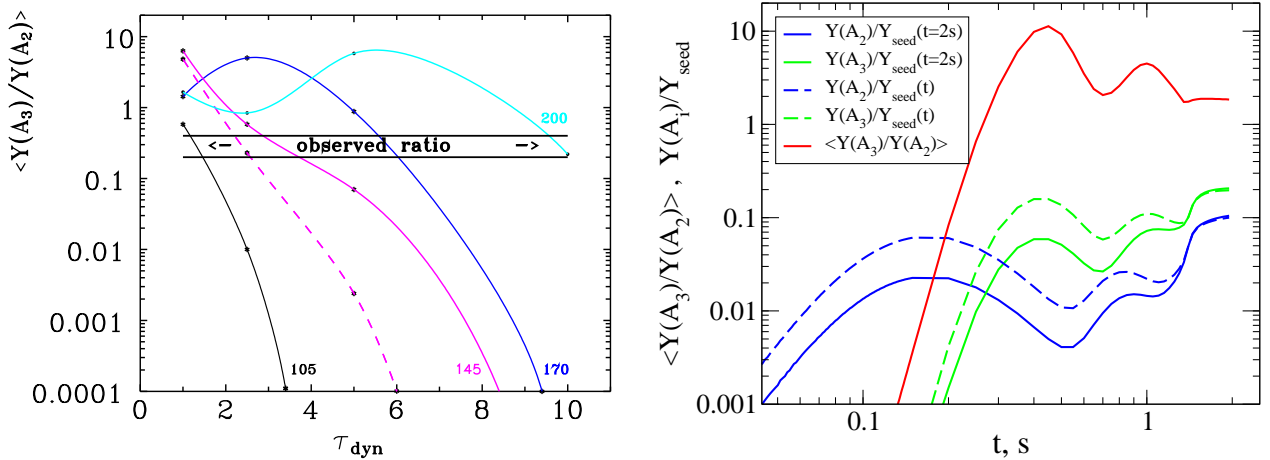


Fig. 11. *Left:* Height of the third abundance peak relative to the second as function of the exponential expansion timescale τ_{dyn} , for different values of the entropy (labels at curves). The solid lines correspond to outflows with a power-law temperature decay following the exponential expansion, while the dashed line shows for comparison the results for $s = 145$ and constant temperature $T_9^f(t > t_0) = T_9^0$ during the second, slow expansion phase. In all cases the outflow was assumed to have an electron fraction of $Y_e = 0.42$ and the transition temperature was taken to be $T_9^f(t_0) = 1$. The band between the two bold horizontal lines marks the observational range. *Right:* Time evolution of the ratio of the third abundance peak to the second peak and of the second and third abundance peaks, $Y(A_2)$ and $Y(A_3)$ (according to the definition in Eq. 11), normalized to the total amounts of seed nuclei, Y_{seed} , at any given time t (dashed lines) and to the seed abundance at the end of the evolution at $t = 2$ s (solid lines), respectively; the different line styles and colors are labelled in the inset box. Note that we consider all nuclei with $Z > 2$ as seeds. The results were computed for $s = 200$, $\tau_{\text{dyn}} = 1$ ms, $Y_e = 0.42$, and $T_9^f(t_0) = 1$. The waves visible in the time evolution of the different quantities reflect the effects of fission cycling in an environment with a very high free neutron density, which is the case for the extreme parameters of this run.

ing with preceding, slower supernova ejecta. On the one hand we considered the temperature and density to reach a lower limit and to remain constant later on. This is equivalent to a constant value of the outer boundary pressure as adopted by Sumiyoshi et al. (2000), Terasawa et al. (2002), and Wanajo et al. (2002) and corresponds to a situation where the homologous outflow is asymptotically decelerated to zero velocity. On the other hand we investigated a

case where the velocity was assumed to make a transition from the linear growth of the wind phase to an asymptotically constant, nonvanishing value, in which case the density decreases with time like t^{-2} and the temperature (for constant radiation entropy) like $t^{-2/3}$.

We have found that for given and constant wind radiation entropy (we explored $s \sim 100$ – $200 k_B$ per nucleon), neutron-to-proton ratio ($Y_e \sim 0.42$ – 0.46), and wind expan-

sion timescale ($\tau_{\text{dyn}} \sim 1\text{--}10$ ms), a strong r-process with production of the third abundance peak depends not only on the value of the transition temperature between the two expansion phases, but also on the evolution of temperature and density during the second, slower stage. In the case of a constant asymptotic temperature and density, the formation of the platinum peak is enabled when the asymptotic temperature value is moderately high ($T_9^0 \sim 0.2\text{--}0.8$). When leaving this range towards lower or higher asymptotic temperatures, the possibility of third-peak formation strongly decreases. This behavior was also seen by Wanajo et al. (2002) and Terasawa et al. (2002) for, as they called them, “freezeout temperatures” or “boundary temperatures” above $T_9^0 \sim 0.4$, but the variation with even lower temperatures remained unexplored in both works.

In our second considered case with power-law decline of $T(t)$ and $\rho(t)$, the strength of the $A \sim 195$ abundance peak compared to the $A \sim 130$ peak turned out to be relatively independent of the transition temperature $T^f(t_0)$ in the interval between about 3×10^8 K and 1.4×10^9 K. For lower transition temperatures the third-peak formation decreases steeply and behaves similar to the case with constant asymptotic temperature and density. This means that the appearance and disappearance of a prominent platinum peak when the constant asymptotic temperature is lowered from $T_9^0 \sim 1$ to $T_9^0 \sim 0.1$, is not observed in the case of a power-law decline of temperature and density during the late wind evolution. Interestingly, both considered cases of late-time expansion behavior also lead to distinctive differences in the abundances of neighboring isotopes of r-process elements. For the power-law time-dependence not only more neutron-rich isotopes are formed but the isotopic distribution is also smoother.

Strong r-processing naturally requires a sufficiently fast expansion in the homologous phase so that charged-particle reactions freeze out before excessive seed production occurs and high neutron-to-seed ratios cannot be reached. Moreover, a relatively rapid temperature decline during the second, slower expansion phase, and at the same time a persistence of sufficiently high neutron number densities ($n_n \gtrsim 10^{24}$ cm $^{-3}$) are favorable for driving the nuclear flow beyond the second abundance peak. For fixed radiation entropy s as assumed in our models, temperature and density are coupled by the relation $s \propto \rho/T^3 = \text{const}$. In this case the asymptotic power-law decrease of both quantities enables third peak formation for a wider range of transition temperatures.

Terasawa et al. (2002) argued that lower asymptotic temperatures reduce the charged-particle reactions, which leads to less seed production and a higher neutron-to-seed ratio, thus causing a better agreement of the r-process yields with the solar abundances. For our calculations, which are based on the idealized two-stage model of the wind expansion, this argument cannot be made. Long before the corresponding asymptotic temperatures (between $T_9 = 0.1$ and $T_9 = 1.4$) are reached, namely already above $T_9 \approx 2$, charged-current reactions become inefficient because of the impenetrability of the nuclear Coulomb barrier for low-energy thermal protons. Instead, the described nucleosynthesis results can be understood by the density and temperature dependence of neutron-captures and nuclear photodisintegration reactions.

Since the (γ, n) -rates decrease steeply with falling temperature, their role diminishes with a lower transition tem-

perature. For sufficiently high neutron densities the still rapid neutron captures force the r-process path towards the neutron-drip line, where the β -decay rates are large. Instead of going through a (γ, n) - (n, γ) equilibrium, the r-processing proceeds now as a quasi-equilibrium of (n, γ) reactions and β -decays, which suggests the term “r β -process”. This situation in outflows that expand supersonically and cool quickly to a few 10^8 K was recently also discussed by Wanajo (2007), who named it “cold r-process”. The formation of the third abundance peak is possible in this situation, provided the neutron-to-seed ratio is large enough, because the β -decays are fast and allow for a quick assembling of heavy nuclei. In contrast, if the exponential expansion makes a transition to a constant temperature that is high, (γ, n) -reactions drive the r-process path towards the valley of stability where the β -decay rates are small and the r-processing therefore slows down. In this case the free neutrons are used up in forming the second abundance peak before any significant third maximum can build up. On the other hand, the power-law temperature decline in the slow expansion phase leads to an efficient r β -process for a wide range of transition temperatures $T_9^f(t_0)$. Because the strength of the third abundance peak then depends only on the neutron density, it becomes relatively insensitive to the value of $T_9^f(t_0)$ between about 0.3 and 1.4. If the transition temperature is even lower, the free neutron density during the slow expansion phase of the outflow is not large enough any more to support a strong r-processing.

In previous investigations (Terasawa et al. 2001, 2002; Wanajo et al. 2002) the complex influence of the late-time outflow behavior was not explored, but it matters when the robustness of abundance yields to variations in the neutrino-driven wind models is discussed, especially in situations where high entropies, low temperatures, and high neutron densities lead to a change of the r-process to an r β -process.

In summary, we therefore conclude that the detailed cooling behavior during the late expansion of supernova outflows can have important consequences for r-process nucleosynthesis. In particular, a slow expansion phase with decreasing temperature and density following a rapid, supersonic initial outflow expansion, is more favorable for a strong r-process than the constant boundary conditions assumed previously (e.g., Wanajo et al. 2001, 2002; Terasawa et al. 2001, 2002). Despite differences in the initial neutron number density by more than two orders of magnitude, such conditions can lead to a fairly robust production of the platinum peak for a wider range of transition temperatures. This is caused by a kind of self-regulation of the quasi-equilibrium of (γ, n) -reactions and β -decays in the r β -process, which leads to roughly the same number of neutron captures per seed nucleus, independent of whether the process proceeds quickly for high neutron densities (in which case the r-process path is closer to the neutron-drip line) or slower in the case of low neutron densities. This might give a hint for the outflow dynamics of neutrino-driven wind ejecta that can enable the uniform production of heavy r-process elements suggested by the abundance patterns observed in metal-poor stars (see e.g., Cowan & Sneden 2006).

For the explored range of parameter values, the r-processing can last 150–200 ms or even longer. This duration is the lower time limit for the formation of heavy elements from iron-group seeds up to the platinum peak. For

entropies s between 100 and $200 k_B$ per nucleon, a solar-like production of the heaviest elements can occur only in the case that the outflow expansion decelerates and a transition from the initial homologous phase to a slower later stage of expansion occurs. In addition, a short or very short exponential timescale ($\tau_{\text{dyn}} \sim 10$ ms for $s = 200$ and $\tau_{\text{dyn}} \sim 1$ ms for $s = 100$) is needed during the homologous expansion, if moderately neutron-rich conditions ($Y_e = 0.42$) are considered. Of course, if the neutron excess decreases, the formation of the third abundance peak requires a higher entropy. These parameter constraints are very similar to those shown in Fig. 10 of Hoffman et al. (1997). This can be understood from the fact that supersonic solutions of the neutrino-driven wind equations as those employed by Hoffman et al. (1997) show approximately homologous expansion ($v \propto r$) only up to some maximum radius, above which the velocity continues to grow significantly less rapidly. Although there is no deceleration as it is caused by a wind termination shock (see Arcones et al. 2007), the slow-down of the expansion of supersonic winds has still some basic similarity to the transition from a rapid first expansion phase to a slower second stage as assumed in our simplified outflow models.

Acknowledgements

Acknowledgements. This work was in part supported by the SNF project No. IB7320-110996 and by the Deutsche Forschungsgemeinschaft through the Transregional Collaborative Research Centers SFB/TR 27 “Neutrinos and Beyond” and SFB/TR 7 “Gravitational Wave Astronomy”, and the Cluster of Excellence EXC 153 “Origin and Structure of the Universe” (<http://www.universe-cluster.de>).

References

- Arcones, A., Janka, H.-Th., & Scheck, L. 2007, *A&A*, 467, 1227
 Arnould, M., Goriely, S., & Takahashi, K. 2007, *Physics Reports*, 450, 97
 Beun, J., McLaughlin, G.C., Surman, R., & Hix, W.R. 2008, *Phys. Rev. C*, 77, 035804
 Bisnovatyi-Kogan, G. S., & Chechetkin, V. M. 1979, *Sov. Uspehi Phys. Nauk*, 127, 263
 Blake, J. B., & Schramm, D. N. 1976, *Astrophysical Journal*, 209, 846
 Blinnikov, S. I., & Panov, I. V. 1996, *Astronomy Letters*, 22, 39
 Buras, R., Janka, H.-Th., Rampp, M., & Kifonidis, K. *A&A*, 2006, 457, 281
 Burbidge, G. R., Burbidge, E. M., Fowler, W. A., & Hoyle, F. 1957, *Rev. Mod. Phys.*, 29, 547
 Burrows, A., Hayes, J., & Fryxell, B. A., 1995, *ApJ*, 450, 830
 Cameron, A. G. W. 2003, *ApJ*, 587, 327
 Cameron, A. G. W., Cowan, J. J., & Truran, J. W. 1983, *Astrophysics and Space Science*, 91, 235
 Cardall, C. Y., Fuller, G. M. 1997, *ApJ*, 486, L111
 Cowan, J. J. & Sneden, C. 2006, *Nature*, 440, 1151
 Cowan, J. J., Thielemann, F.-K., & Truran, J. W. 1991, *Phys. Rep.*, 208, 267
 Freiburghaus, C., Rosswog, S., & Thielemann, F.-K. 1999, *ApJ*, 525, L121
 Gear, C. W., 1971, *Numerical Initial Value Problems in Ordinary Differential Equations* (Englewood Cliffs, New Jersey: Prentice-Hall)
 Goriely, S., Demetriou, P., Janka, H.-Th., Pearson, J. M. & Samyn, M. 2005, *Nuclear Physics A*, 758 587c
 Hillebrandt, W. 1978, *Space Sci. Rev.*, 21, 639
 Hoffman, R. D., Woosley, S. E., & Qian, Y.-Z. 1997, *ApJ*, 482, 951
 Imshennik, V. S. 1992, *Astronomy Letters*, 18, 194
 Imshennik, V. S., Litvinova I. Yu. 2006. *Atomic Nuclei*, 69, 660.
 Janka, H.-Th., & Müller, E. 1995, *Physics Reports*, 256, 135
 Janka, H.-Th., & Müller, E. 1995, *ApJ*, 448, L109
 Kratz, K.-L., Bitouzet, J.-P., Thielemann, F.-K., Möller, P., & Pfeiffer, B. 1993, *ApJ*, 403, 216
 Kuroda, T., Wanajo, S., & Nomoto, K. 2008, *ApJ*, 672, 1068
 Lattimer, J. M., & Schramm, D. N. 1974, *ApJ*, 192, L145
 Lattimer, J. M., Schramm, D. N., 1976, *ApJ*, 210, 549
 Meyer, B. S., Mathews, G. J., Howard, W. M., Woosley, S. E., & Hoffman, R. D., 1992, *ApJ*, 399, 656.
 Nadyozhin, D. K., Panov, I. V., & Blinnikov, S.I. 1998, *A&A*, 335, 207.
 Nadyozhin, D. K., & Yudin, A. V. 2004, *Astronomy Letters*, 30, 697
 Otsuki, K., Tagoshi, H., Kajino, T., & Wanajo, S. 2000, *ApJ*, 533, 424
 Panov, I. V., Blinnikov, S. I., & Thielemann, F.-K. 2001a, *Astronomy Letters*, 27, 1
 Panov, I. V., Freiburghaus, C., Thielemann, F.-K. 2001b, *Nucl. Phys. A*, 688, 587
 Panov, I. V., Chechetkin, V. M. 2002, *Astronomy Letters*, 28, 476
 Panov I. V., Thielemann F.-K., 2003a, *Nucl. Phys. A*, 718, 647
 Panov, I. V. 2003b, *Astronomy Letters*, 29, 163
 Panov, I. V., Kolbe, E., Pfeiffer, B., Rauscher, Th., Kratz, K.-L., Thielemann, F.-K. 2005, *Nuclear Physics A*, 747, 633
 Qian, Y.-Z., & Woosley, S.E. 1996, *ApJ*, 471, 331
 Qian, Y.-Z., & Wasserburg, G. J. 2000, *Physics reports*, 333, 77
 Rauscher, T., Thielemann, F.-K., & Kratz, K.-L. 1997, *Nucl. Phys.*, A 621, 331c.
 Rauscher, T., & Thielemann, F.-K. 2000, *Atomic Data Nucl. Data Tables*, 75, 1
 Symbalisty, E. M. D., & Schramm, D. N. 1982, *Astrophysical Letters*, 22, 143
 Seeger, P. A., Fowler, W. A., & Clayton, D. D. 1965, *ApJS*, 11, 121
 Sumiyoshi, K., Suzuki, H., Otsuki, K., Terasawa, M., & Yamada Sh. 2000, *Publ. Astron. Soc. Japan.*, 52, 601
 Takahashi, K., Wittl, J., Janka, H.-T. 1994, *A&A*, 286, 857
 Takahashi, K., Janka, H.-T. 1997, *Proceedings of an int. conf. Origin of matter and evolution of galaxies in the universe '96*. Atami, Japan, 18-20 January 1996, Singapore: World Scientific, 1997, edited by T. Kajino, Y. Yoshii, and S. Kubono, p. 213.
 Terasawa, M., Sumiyoshi, K., Kajino, T., Mathews, G. J., & Tanihata, I. 2001, *ApJ*, 562, 470
 Terasawa, M., Sumiyoshi, K., Yamada, S., Suzuki, H., & Kajino, T. 2002, *ApJ*, 578, L137
 Thompson, T. A., Burrows, A., & Meyer, B. S. 2001, *ApJ*, 562 887
 Tomàs, R., Kachelrieß, M., Raffelt, G., Dighe, A., Janka, H.-T., & Scheck, L. 2004, *Journal of Cosmology and Astroparticle Physics*, 09, 015
 Wittl, J., Janka, H.-Th., Takahashi, K., & Hillebrandt, W. 1993, In *Nuclei in the Cosmos-IX*, Eds. F. Käppeler, K. Wisshak (Bristol and Philadelphia: Inst. of Phys. Publ.), p. 601
 Wittl, J., Janka, H.-T., & Takahashi, K. 1994, *A&A*, 286, 841
 Woosley, S. E., & Hoffman, R. D. 1992, *ApJ*, 395, 202
 Woosley, S. E., Wilson, J. R., Mathews, G. J., Hoffman, R. D., Meyer, B. S. 1994, *ApJ*, 433, 229
 Wanajo, S., 2007, *ApJ*, 666, L77
 Wanajo, S., & Ishimaru, Y. 2006, *Nuclear Physics A*, 777, 676
 Wanajo, S., Itoh, N., Ishimaru, Yu., Nozawa, S., & Beers, T. C. 2002, *ApJ*, 577, 853
 Wanajo, S., Kajino, T., Mathews, G. J., & Otsuki, K. 2001, *ApJ*, 554, 578